scientific reports

Check for updates

OPEN

Enhanced hemocompatibility, antimicrobial and anti-inflammatory properties of biomolecules stabilized AgNPs with cytotoxic effects on cancer cells

Azam Chahardoli[1]✉, Farshad Qalekhani[2], Pouria Hajmomeni[2], Yalda Shokoohinia[2,3]✉ & Ali Fattahi[2,4]✉

In the current research, we developed a safe method using Iranian yarrow extract for the synthesis of silver nanoparticles (IY-AgNPs) as reducing and stabilizing agents in different conditions. The prepared and stabilized IY-AgNPs under optimal conditions were characterized using FT-IR, XRD, TEM, and UV-vis techniques. Also, the blood-clotting, hemolytic, antioxidant, bactericidal and, fungicidal properties, cytotoxicity effects and inhibition of protein denaturation efficiency of IY-AgNPs were assessed in vitro. The stabilized IY-AgNPs with spherical shape and an average particle size of 19. 25 ± 7.9 nm did not show any hemolytic potential below 1000 µg/mL. These hemo-compatible NPs showed good blood-clotting ability by reducing clotting time (6 min relative to the control). These particles excellently inhibited the denaturation of bovine serum albumin (BSA) by 69.3–80.7% at concentrations ranging from 31.25 to 500 µg/mL compared to a reference drug. The outcomes showed that the IC50 values of IY-AgNPs were below 12.5 µg/mL against A375 cells and between 25 and 50 µg/mL against MCF-7 cancer cells. In addition, IY-AgNPs were bactericidal against *Escherichia coli*, *Pseudomonas aeruginosa* and *Staphylococcus aureus* (especially), and were fungicidal against *Candida albicans*. Biosynthesized IY-AgNPs indicated a significant antioxidant activity (63.2%) at a concentration of 350 µg/mL. These attained results suggested that bio/hemo-compatible IY-AgNPs may be a promising candidate for applications in the medicinal fields (particularly for wound healing) as anti-bleeding, antimicrobial, antioxidant, anti-inflammatory, and anticancer agents.

Keywords Anti-bleeding, Anti-inflammatory effect, Antioxidant, Cancer cells, Hemocompatibility, Microbiocidal activity

The genus Achillea has many medicinal species with numerous therapeutic benefits[1]. Achillea is referred to the Achilles, which was used by Iliad to treat the soldiers' wounds in the literary Trojan War[2]. These plants are reported as antioxidant, antitumoral, antibacterial, antiulcer, anti-inflammatory, antihyperlipidemic, antihypertensive, anti-spasmodic, diaphoretic, diuretic, and emmenagogic agents and have been used for gastrointestinal disorders, treatment of rheumatic, pneumonia and hemorrhagepain and effective in wound healing in traditional literature[3–6]. Achillea includes Iranian yarrow or Bumadaran in the Persian language (*Achillea wilhelmsii* C. Koch), has chemical components comprising flavonoids, polyphenols, alkaloids (achilleine), sesquiterpenoids (lactones), monoterpenoids, cineol, camphene, camphor, α- and β-pinen, thymol, thujene, caryophyllene, borneol and rutin[3,5,7]. Anti-cancer effects of Iranian yarrow extract on breast, prostate, and HeLa cervical cancer cells have been reported in previous studies[8–10]. The anti-inflammatory properties of these plants were applied for the treatment of skin inflammations and wound healing[11]. Furthermore, the yarrow

[1]Department of Biology, Faculty of Science, Razi University, Kermanshah 6714414971, Iran. [2]Pharmaceutical Sciences Research Center, Health Institute, Kermanshah University of Medical Sciences, Kermanshah, Iran. [3]Ric Scalzo Botanical Research Institute, Southwest College of Naturopathic Medicine, Tempe, AZ, USA. [4]Medical Biology Research Center, Health Technologies Institute, Kermanshah University of Medical Sciences, Kermanshah, Iran. ✉email: a.chahardoli@razi.ac.ir; shokoohinia@scnm.edu; a.fatahi.a@gmail.com

leaf extract used to stop wound bleeding, stimulate healing of minor wounds, ulcerations, sores and combat interior bleeding in traditional medicine[12].

In the current work, we synthesized silver nanoparticles (AgNPs) using the reducing power of phytochemical compounds from Iranian yarrow to evaluate their biological activities (bio-compatibility and hemo-compatibility). Compared to the unfavorable chemical procedures, the green method uses non-toxic components with medical value as reducing and stabilizing agents, making it safe for medical applications such as anticancer, antibacterial and drug delivery systems[13]. Therefore, the surface coating of nanoparticles by non-toxic phytochemicals could make them safe and biocompatible for healthcare and biomedical targets[14]. Among the biosynthesized nanoparticles, AgNPs have exhibited antimicrobial, antiviral, anticancer, anti-inflammatory, antioxidant, anti-angiogenesis, and anti-platelet activities[15]. However, the most of previous papers focused on the biologically synthesis of AgNPs using various plant extracts and evaluation of some of their biological properties. To date, little attention has been paid to the effect of plant phytochemical present on the surface of NPs on the hemo/biocompatibility of biogenic AgNPs and their interaction with blood cells and components. Once, NPs enter the bloodstream, may come into contact with blood cells and plasma proteins, triggering pathophysiological processes. Therefore, the hemocompatibility of AgNPs should be carefully investigated. Although, the comparisons of NPs effects on blood compounds are very difficult due to their different sizes and coatings. Based on ISO-10993-4, the safety assessment of medical devices should include red blood cells, platelets, hematology, coagulation and complement systems[16]. Among body fluids red blood cells (RBCs) are the major cellular component and once AgNPs get exposed to the bloodstream it causes RBC lysis, the physiochemical changes in their membrane and induces severe toxicological effects in the system[17]. Loss of platelet function, which is important for primary hemostasis, can lead to bleeding and thrombotic disorders. Similar to secondary hemostasis, the plasma coagulation cascade is responsible for blood clotting and is activated by platelets[18]. Hence, AgNPs used for such applications should be suitably surface-modified to establish an ecofriendly contact with the human system[17].

Besides, AgNPs have displayed significant potential in cancer research. Cancer is a complex and very severe genetic disease characterized by abnormal and uncontrolled cell division, and cancer cells spread throughout the body using the blood and lymphatic systems. Although chemotherapy and radiotherapy are accepted methods of cancer treatment, these protocols destroy both normal and cancer cells, and the chemotherapeutic agents available have harmful side effects. To overcome these drawbacks, protocols that have as few side effects as possible, are biocompatible, and cost-effective must be implemented. Therefore, AgNPs have been widely used to improve nanodevices and therapeutic formulations for cancer diagnosis and treatment due to their special catalytic, bactericidal, therapeutic efficacy and stability[19]. The cytotoxicity of plant-based NPs against cancer cells depends on the size and shape of NPs as well as the exposure time and dosage[20]. AgNPs can easily penetrate to cells through the cell membrane and cell wall and then lead to the integration of membrane bilayer, production of excessive reactive oxygen species (ROS), damage to proteins and DNA, which leads to cell death by stimulation of necrotic and apoptotic cell death pathways[21].

These NPs have been used widely in medical devices due to their known antibacterial and antifungal properties for preventing infection. Various healthcare products, for example blood bags, wound dressings, biomaterial implants, stents, and catheters require microbiocidal properties to prevent infection and biofouling[13]. These NPs, due to their conjugation with sulfur in sulfhydryl and other sulfur-based functional groups (in bacterial respiratory enzymes) have been reported to be one of the most important antibacterial, antifungal, and antiviral agents that have been widely used in the development of surface modification strategies as drug carriers in biomedical applications. AgNPs also bind to phosphorus-containing components such as DNA, thereby preventing its replication process. They also inhibit the antioxidant system, which handles free radicals, inactivate vital proteins and other cellular functions and ultimately cause irreparable damage to cells[22]. Due to this, AgNPs play a key role in wound healing as their antibacterial properties create a favorable environment for tissue regeneration and wound closure, making them a valuable component of modern wound care materials[23]. Using phytochemicals in yarrow plant extracts (with anti-bleeding properties and stimulating wounds healing in infections) as a stabilizing and capping layer around AgNPs can synergistically enhance antimicrobial activity and wound healing[24,25]. These NPs with excellent antibacterial effects against a broad range of bacteria are a proper and attractive alternative to antibiotics and can inhibit multidrug resistance bacteria without any toxicity to animal or human cells, which are employed as novel compounds to prevent multidrug-resistant microorganisms[25,26].

In addition, the antimicrobial activity of AgNPs, these particles with anti-inflammatory potential can accelerate wound healing and can reduce or eliminate the inflammation[27,28]. Inflammation is the immune system's protective response of the body to infection, injury, or destruction caused by microbial agents, noxious chemical or physical trauma, which characterized by disturbed physiological functions, heat, redness, swelling and pain, increase of protein denaturation and increase of membrane alteration and vascular permeability[29–31]. Inflammation and hemostasis processes are initiated by releasing clotting factors, blood components and platelets, in the wound or injury site[32]. The in-vitro evaluation of red blood cells (RBCs) hemolysis is usually applied for screening anti-inflammatory activity of drugs, which these drugs with stabilize the plasma membrane of RBCs lead to inhibition of heat-induced or hypo-tonicity-induced hemolysis[31]. The commonly used drugs for inflammation are non-steroidal drugs, which especially have various adverse effects on the gastric irritation and usually result in the formation of gastric ulcers[33]. Thus, AgNPs with anti-inflammatory activity may be a promising agent in the treatment of inflammation diseases. In fact, AgNPs by preventing microbial infection in wounds lead to accelerating the wound healing process owing to their angiogenic and anti-inflammatory properties[32]. Therefore, in the present research in addition to biosynthesis of AgNPs from Iranian yarrow extract, their characterization were analyzed by UV-Vis, X-ray diffraction (XRD), Fourier transform infrared (FTIR), and Transmission Electron Microscopy (TEM). Moreover, we focused on the evaluation of their antibacterial

and anti-inflammatory activities, as well as their effects on whole blood clotting time and RBC hemolysis and cytotoxicity against human melanoma and breast cancer cells, which is a rare combination of properties in a single study. Thus, cost-effective, easy and eco-friendly synthesized IY-AgNPs with excellent hemocompatibility, antioxidant, antibacterial, anticancer properties may be able to solve the problems and side effects of common chemical drugs and contribute significantly to the design of therapies and drug delivery systems to treat cancers, infections and wounds.

Materials and methods

Materials

Silver nitrate ($AgNO_3$), 2,2-diphenyl-1- picrylhydrazyl (DPPH), Methanol, Calcium chloride ($CaCl_2$), 3-(4,5-dimethylthiazol-2-yl)-2,5-diphenyl tetrazolium (MTT) and fetal bovine serum (FBS), Mueller– Hinton agar and broth, dimethyl sulfoxide (DMSO) were purchased from Sigma (St Louis, MO, USA). Moreover, Dulbecco's modified Eagle's medium (DMEM-F12) was purchased from Gibco (Gibco, Grand Island, NY, USA). All other chemicals were analytical reagent grade and used without any further purification, purchased from Merck, Germany. All tested microorganisms were purchased from Pasteur institute, Tehran, Iran.

Preparation of yarrow aerial part extract

Iranian yarrow (IY) was collected from a mountain at an altitude of 1600 m in Kermanshah Province, Iran (Terazag Abdullah village - Gharb city, Islamabad) in spring. This plant species was documented by Dr. Nastaran Jalilian (Forests Rangelands, and Research Department, Kermanshah, Iran). Plant aerial parts were separated and washed with distilled water and then, dried at room condition and processed into powder in a blender. Plant extraction was carried out using sonication of 10 g of plant powder in 100 ml of deionized water at 45 °C for 30 min in an ultrasonic bath. This mixture, after initial filtration, was centrifuged at 5000 rpm for 40 min. The obtained watery extract was put away at 4 °C for future analysis.

Syntheses of IY-AgNPs

In order to synthesize IY-AgNPs, primarily, $AgNO_3$ solution at a concentration of 1 mM was produced in distilled water and combined with 10 mL of aqueous extract of IY. The blend was incubated at different temperatures of 37, 50, and 70 °C and pH of 5, 7, and 10. A color alter of the response blend from pale yellow to brown appeared the arrangement of IY-AgNPs.

Characterization pathways of IY-AgNPs

UV–Vis detection

UV–Vis detection was performed on the obtained suspensions by dilutiing in deionized water. The absorptions of IY-AgNPs solution at different time intervals were scanned at a wavelength range of 200–700 nm on a spectrophotometer (Specord 210 plus, Analytik Jena, Germany) using a quartz cuvette with a 3 cm path length. For the next analysis, synthesized IY-AgNPs were purified by repeated centrifugation and re-suspension (3 times) of the reaction mixture at 10,000 rpm for 30 min. The obtained pellet was freeze-dried.

Fourier transform infrared (FTIR) spectroscopy

FTIR analysis of both the IY extract and IY-AgNPs was performed using the potassium bromide pellet method in the spectral range of 400–4000 cm^{-1} on IR Prestige-21 Shimadzu Spectrometer, Kyoto, Japan. This detection method is beneficial to detect the reducing and stabilizing role of the functional groups in phytochemicals present within the IY extract in the synthesis process of IY-AgNPs.

Morphologic and size analysis of IY-AgNPs

Morphological and size analysis of IY-AgNPs was detected by Transmission electron microscopy (TEM) on a Zeiss-EM10C microscope, Germany, with an acceleration voltage of 100 kV.

The X-ray diffraction (XRD) spectrum

XRD analysis for the detection of crystalline nature of powdered IY-AgNPs was recorded by X-ray diffractometer (X'PertPro, Panalytical, Holland), which operated at 40 kV and 30 mA using Cu K^{-1} radiation. Data were analyzed in a 2θ scanning range of 20°- 80°.

Energy-dispersive X-ray spectroscopy (EDS)

The elemental compositions of IY-AgNPs were analyzed by the EDS detector incorporated in SEM system (SEM/EDX- Bruker Nano GmbH Berlin, Germany).

Biological properties

Cell culture

The human melanoma cancer cell line (A375) was purchased from the Pasteur Institute of Iran (Tehran, Iran) and the breast cancer cell line (MCF-7) was obtained from the Cell Line Bank of Kermanshah University of Medical Sciences (Kermanshah, Iran). Cells were cultured in DMEM-F12 cell culture medium (including10% (v/v) FBS and 1% penicillin and streptomycin) at 37 °C with 5% CO_2 and 95% atmospheric humidity until reaching an appropriate density.

Cell viability against IY-AgNPs

The cytotoxic effects of IY-AgNPs on viability of A375 and MCF-7 were examined by MTT (3-(4, 5-dimethyl-2-thiazol)-2, 5-diphenyl-2 H-tetrazolium bromide) procedure. The target cells at concentration of 1×10^5 cells/

mL were seeded in 96-well plates and incubated at 37 °C with 5% CO_2. These cells in triplicate were treated by IY-AgNPs and IY-extract at concentrations of 0, 6.25, 12.5, 25, 50, and 100 µg/mL. Plates containing treated cells were placed in a 5% CO_2 incubator at 37 °C for 48 h. After the exposure time and washing of all cells, MTT (10 mg/mL) was included to each well and prepared plates were brooded for 3 h at 37 °C. Subsequently, DMSO (dimethyl sulfoxide) was included to break up the formazone crystals. Finally, an ELISA plate reader (Bio-Rad, model 680, USA) was used to document the absorbance of the exposed cells was at 540 nm and 630 and calculate the cell viability (%) relative to the untreated control cells.

Antioxidant effect of IY-AgNPs

The antioxidant effect of IY-AgNPs was assayed by determining their inhibitory potential against 2,2-diphenyl-1-picrylhydrazyl (DPPH) free radical. IY-AgNPs and IY-extract at concentrations of 150, 200, 250, 300, and 350 µg/mL were prepared in different test tubes. For performance of this test, one mL of DPPH fresh solution (0.1 mM in methanol) was added to each tube containing samples and vortexed thoroughly. The prepared reaction mixture in triplicate was incubated for 30 min in the dark condition. After incubation, the absorbance of (Abs.) samples was documented at 517 nm against a blank. The control sample contained DPPH in methanol. The percentage of DPPH radical inhibition was estimated using the following procedure:

$$\text{Percentage of inhibition} = \text{Abs. control - Abs.sample/Abs. control} \times 100$$

Fungicidal and bactericidal effects of IY-AgNPs

Minimum inhibitory concentration (MIC), minimum fungicidal concentration (MFC), and minimum bactericidal concentration (MBC) were tested by the standard broth microdilution method to determine the fungicidal and bactericidal effects of IY-AgNPs. Stock solution (400 µg/mL) of IY-AgNPs was prepared, and as the serial dilution was added into each well containing a100 µL of Muller Hinton broth in 96 -well plates, followed by adding 1×10^8 CFU/mL of the fungal (*Candida albicans*) or bacterial (*Escherichia coli* ATCC 25922, *Pseudomonas aeruginosa* ATCC 27853 and the gram-positive strain *Staphylococcus aureus* ATCC 29213) cells. The treated plates were incubated at 37 °C for 24 h. The MFC and MBC were defined as the lowest concentration of IY-AgNPs, which completely prevent fungal and bacterial growth, and were performed after the MIC test by culturing a drop of fungal or bacterial broth with no visual growth on the agar medium.

Hemocaompatibility

All blood experiments were performed in accordance with relevant guidelines and regulations. The all methods in the current study were approved by the Ethical Committee of the National Institute for Medicinal Research Development (ethical code: IR.NIMAD.REC.1397.537). Also, we confirm that informed consent was obtained from all participants (25–35 years old healthy adult volunteers) in accordance with the Declaration of Helsinki.

Hemolysis assay

Hemolysis assays were determined on the blood of three healthy donors. Blood testing solution was prepared by centrifugation at 1500 rpm with three repeated washing using 0.9% saline solution. Then, the obtained RBC was re-suspended (10% v/v) in saline solution. The diluted blood (200 µL) was added to IY-AgNPs and IY extract solution (200 µL) at various concentrations of 62.5, 125, 250, 500 and 1000 µg/mL and then incubated at 37 °C for 60 min. After incubation time, all samples (in triplicate) centrifuged at 5000 rpm for 10 min and the supernatants were transferred into 96 well plates and finally, the optical density (OD) of all samples (in triplicate) recorded at 540 nm in Eliza reader. The normal saline and Triton X-100 (1%) were used as a negative (0% hemolysis) and positive (100% hemolysis), respectively. The percentage of hemolysis was estimated as follows: The hemolytic effect of each:

$$\text{Hemolysis effect } (\%) = (\text{OD each samples} - \text{ OD negative control})/(\text{OD positive control} - \text{OD negative control}) \times 100$$

Clotting time assay

Blood clotting time assay performed using blood provided from healthy volunteers based on described literature with slight modifications[34]. Collected blood was mixed with anticoagulant agent acid citrate dextrose at a ratio of 9:1. In order to, 100 µL of IY-AgNPs solution at different concentrations of 250, 500, and 1000 µg/mL was mixed with 180 µL of citrated human blood in a microtube. Then, $CaCl_2$ solution (0.1 M) was added to the prepared samples (in triplicate) to reverse anticoagulation effects of citrate sodium at certain times. Subsequently, the formation of the clot was examined by inversion of the tubes and the time in which the blood samples held their weights upon the tubes' inversion was determined as clotting time compared to a control (normal saline).

In vitro anti-inflammatory activity assay

Membrane stabilization strategy

The anti-inflammatory effect was considered using the membrane stabilization process. The obtained fresh human blood after 15 min centrifugation at 5322 RCF (×g) were washed three times with saline. The collected red blood cells (RBCs) were suspended in saline to achieve a concentration of 10% (v/v). The test samples were prepared at concentrations of 31.25, 62.5, 125, 250 and 500 µg/mL in saline (in triplicate). Afterward, 1 mL of RBC suspension was combined with 1 mL of different concentrations of IY-AgNPs, diclofenac sodium (as a standard drug) and saline (as a control). All blends were brooded for 30 min in a water bath (at 56 °C) and after that cooled to 25 °C. Finally, the absorbance of these samples (in triplicate) was record at 560 nm after 5 min centrifugation at 5322 RCF (×g) and the activity of membrane stabilization was calculated as takes after:

$$\text{Membrane stabilization activity } (\%) = (\text{Abs.control} - \text{Abs.sample})/\ (\text{Abs.control}) \times 100$$

Protein denaturation inhibition

Inhibition of protein denaturation by IY-AgNPs was tested using a slight modification of the previously described method[35]. Bovine serum albumin (BSA 1%) solution in Tris-buffer, (pH 6.5) was added to sample solutions (31.25, 62.5, 125, 250 and 500 µg/mL) in water at ratio 450:500 µL. The prepared mixture in triplicate was incubated initially for 30 min at 37 °C and then was heated for 20 min at 70 °C. Thereafter, samples were cooled down, and their absorbance was documented at 660 nm. The standard drug was diclofenac sodium (DS), and control was the mixture of BSA and water. The extent of albumin denaturation inhibition was estimated as follows:

$$\text{Inhibition percentage of BSA denaturation} = (\text{Abs.control} - \text{Abs.sample})/\ (\text{Abs.control}) \times 100$$

Statistical analysis

All data were statistically analyzed using the SPSS 16.0 software package (SPSS, Inc., Chicago, IL, USA). One-way analysis of variance (ANOVA) followed Tukey's multiple comparisons post hoc test was applied for all data obtained from the various experiments (in triplicates). Data were presented as the mean ± standard error and statistical significance was acceptable to a level of $p < 0.05$. Also, the t-test was used to determine significant differences between the data of any two groups. Furthermore, the TEM data presented as histogram were analyzed using Origin Pro 16 software to determine the average particle size distribution.

Results and discussions

Synthesis of IY-AgNPs

The synthesis of AgNPs was performed under green reaction using IY-extract at different conditions. The IY-extract is very rich in biomolecules, including sesquiterpenoids (leucodin, wilhemsin, wilhelmsolide, artecanin, artecaninhydrate, artemargyinolide B, chloroklotzchin, hanphyllin), flavonoids (penduletin, artemetin, salvigenin, santoflavone (isoschaftoside, vicenin, isovitexin) and phenolic acid of chlorogenic acid[36], which can be reduced Ag ions to IY-AgNPs and can be used as capping agent on the surface of formed NPs. Therefore, IY-extract acts as a strong reducing and capping agent in the synthesis of IY-AgNPs and affects their physicochemical properties as well as their biological applications. The formation of colloidal IY-AgNPs was confirmed initially by the color change of the reaction solution to dark brown color and UV–vis spectroscopy.

Characterization

UV–Vis spectroscopy

The formation of IY-AgNPs in dark conditions at different temperatures and pH was examined by UV–Vis spectrophotometry at regular time intervals (Fig. 1). Two important parameters, including temperatures and pH, which can affect the synthesis of IY-AgNPs and their size, shape, and morphology, were evaluated in the current study. Different pH, 5, 7, and 10, and temperatures of 37, 50, and 70 °C, alone did not affect the formation of IY-AgNPs in reaction time (2–4 h). Also, in the pH value 5 at temperatures 37, 50 and 70 °C, there was no significant peak in the absorption spectra, declaring that there was no formation of NPs, but in the pH value 7 (Fig. 1A–D), the formation of IY-AgNPs occurred at temperature 70 °C in the reaction time 2 h (Fig. 1D). The maximum absorption peak in pH 7 at a temperature of 70 °C obtained around 432 nm (Fig. 1D), which confirms the formations of Ag-NPs. When the pH value was increased to 10, the formation of IY-AgNPs was occurred at temperatures 37, 50, and 70 °C (Fig. 1E–H) in the first few minutes of the reaction, but the sharp and intense SPR peak was observed for pH 10 and temperature 70 °C by maximum absorption peak 400 nm at reaction time 2 h

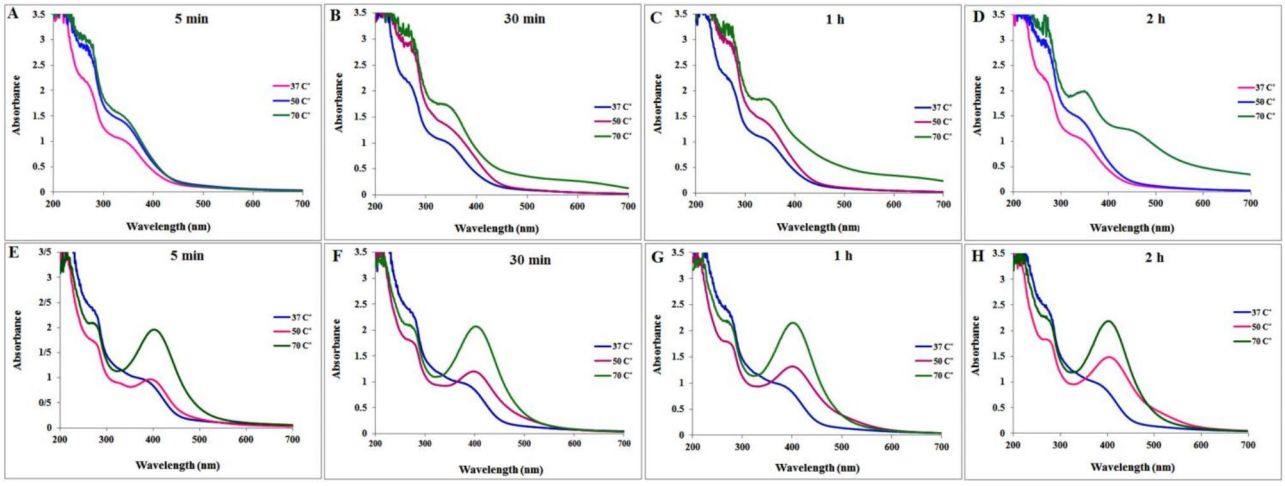

Fig. 1. UV–Vis spectra of IY-AgNPs at different pH 7 (**A**–**D**) and pH 10 (**E**–**H**) under different temperatures of 37, 50, and 70 °C at various time intervals.

(Fig. 1H). However, there was only a small blue shift, which with an increase in temperature, the absorption peak shifted towards a lower wavelength from 404 to 400 nm. These results suggest that the size of the synthesized IY-AgNPs decreases with increasing temperature, which may be due to the effect of higher temperatures on quicker reaction rate. The intensity of SPR peaks for AgNPs synthesized at temperatures of 37 and 50 °C was lower than temperature of 70 °C, which can be owing to incomplete reaction or bigger-sized particles. Therefore, the optimum condition for synthesizing of small IY-AgNPs was achieved at pH 10 and a temperature of 70 °C (Fig. 2A). The UV–Vis spectra of IY-AgNPs obviously show a strong absorption band at 400 nm. An increase in absorbance was detected over time, which demonstrated an increase in the formation of IY-AgNPs.

The role of functional groups in the synthesis of IY-AgNPs

The FT-IR Spectra of IY-AgNPs and IY extract are shown in Fig. 2B. In the IR spectrum for IY extract, important bands appeared at 3383, 2932, 1616, 1400, and 1072 cm^{-1}, which were shifted to the obtained bands at 3441, 2924, 2855, 1638, 1497, and 1084 cm^{-1} in the IR spectrum of IY-AgNPs. A broad band detected at 3441 cm^{-1} was assigned to OH stretching groups of alcohols and phenols.

The C–H vibrational stretching bands of alkanes and O–H stretching bands of carboxylic acids appeared at 2924and 2855 cm^{-1}. The band around 1638 cm^{-1} is assigned to the primary N–H bend of amines, whereas the band at 1497 correspond to the C–C stretch of aromatics and N–O asymmetric stretch of nitro compounds. The C–N stretch peak of aliphatic amines and C–O stretch peak of alcohols, carboxylic acids, esters, and ethers appeared at 1084 cm^{-1}. Therefore, the functional groups such as N–H, C–N, and C–O are present in amino acids, proteins, flavonoids, and pigments that can be involved in the plant extract for the reduction of silver ions to AgNPs[37].

Morphology and size of IY-AgNPs

The obtained images of IY-AgNPs by TEM analysis are shown in Fig. 3A,B. The TEM images revealed that IY-AgNPs are spherical in morphology. Also, this analysis exhibited that the IY-AgNPs with a uniform distribution had a size in a range of 4–39 nm and an average particle size of 19. 25 ± 7.9 nm (Fig. 3C).

Crystalline nature of IY-AgNPs

The XRD pattern of IY-AgNPs is shown in Fig. 4A. The strong peaks around 38.29°, 44.22°, 64.60°, and 77.47° which appeared at 2θ values, corresponding to the presence of (111), (200), (220), and (311) crystallographic planes, respectively. The XRD patterns established the crystalline and face-centered cubic (FCC) nature of IY-AgNPs, which was in accordance with the standard pattern of metallic silver (JCPDS File No. 04-0783). The calculated average crystallite size of IY-AgNPs was 8 nm by Debye–Scherer's equation ($d = 0.9\,\lambda/\beta\cos\theta$).

EDX analysis is commonly known as a semiquantitative method for identifying elements in biosynthetic NPs. The EDX spectrum in Fig. 4B displays the elemental composition profile of the IY-AgNPs. The spectrum shows silver (Ag), carbon (C), oxygen (O), and nitrogen (N) elements (Fig. 4B). The composition of Ag, C, O, and N in NPs was 63.72%, 12.40%, 8.79%, and 3.14% respectively, by weight and atomic percentage of 21.61%, 37.76%, 20.11% and 8.19% respectively. The EDX pattern confirmed the presence of the most intense peaks of elemental Ag at 3 keV. Also, other Ag peaks were below 1 Kev. In addition, the signals of C, O, and N can be seen before 1 Kev, which confirmed the presence of IY extract compounds as reducing and capping agents linked to the surface of IY-AgNPs. The Cl (chlorine) peak with a percentage weight of 11.95% may be from the chlorine group found in the IY extract compounds.

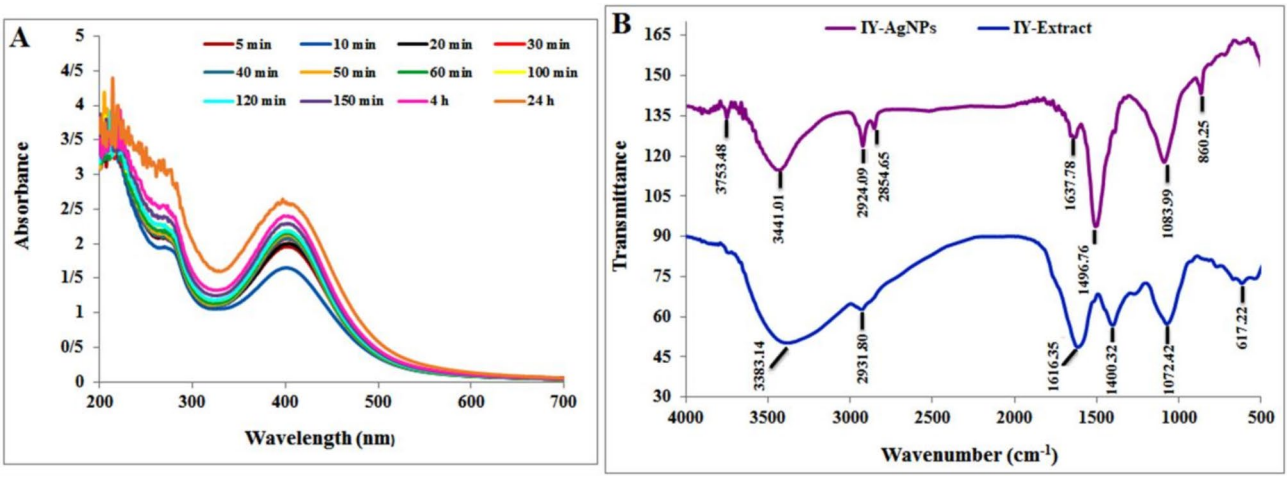

Fig. 2. (**A**) UV–Vis spectra of IY-AgNPs at pH 10 and temperatures 70 °C in the different time intervals, and (**B**) FT-IR spectra of IY-extract and IY-AgNPs.

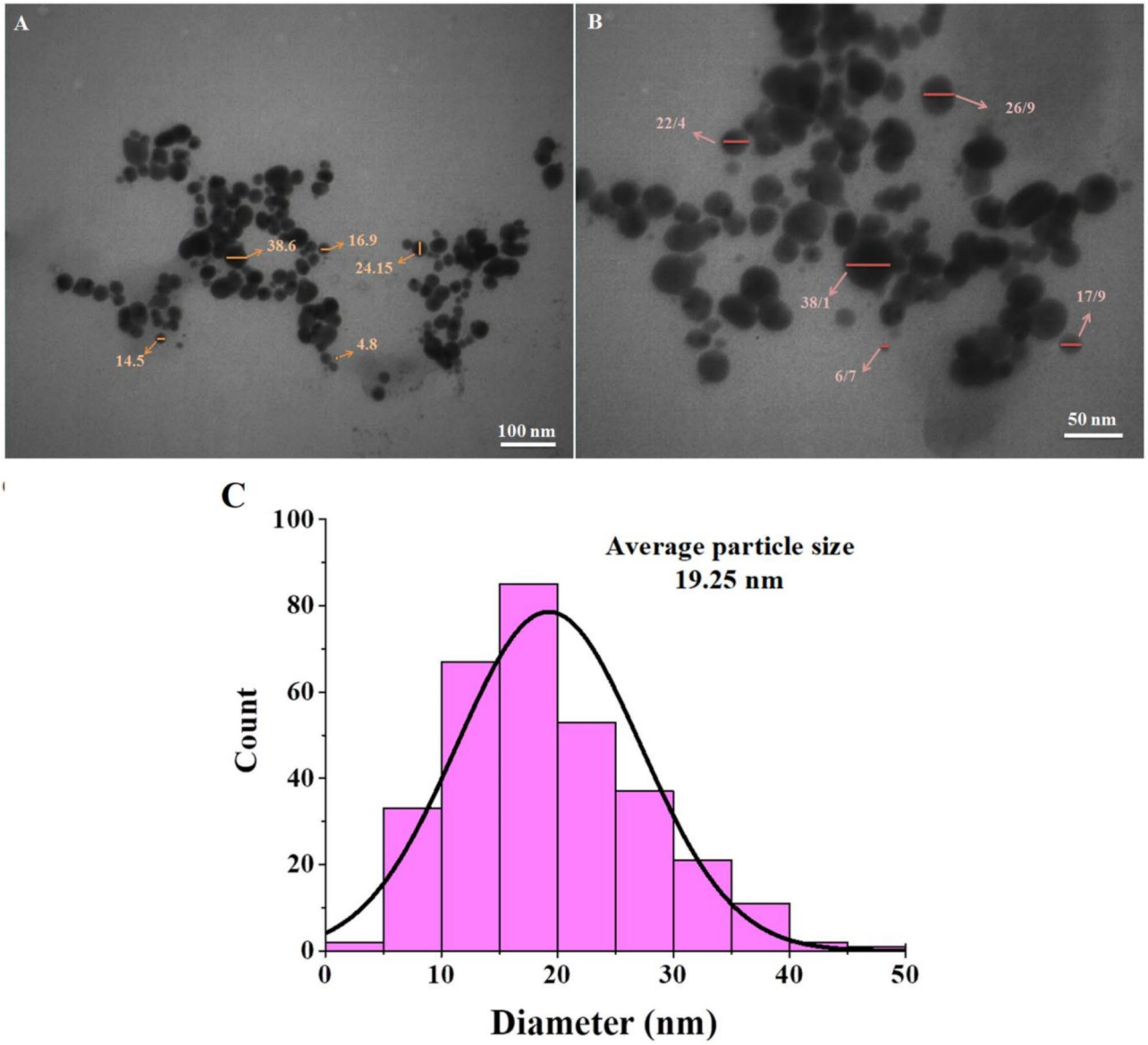

Fig. 3. TEM images at different magnification (**A**,**B**) and particle size distribution histogram (**C**) of IY-AgNPs.

Evaluation of in vitro whole blood clotting and anti-hemolytic activity

Hemostasis, blood clotting, and coagulation refers to the process that inhibits blood loss and bleeding. This process is regulated in the endothelial lining of blood vessels, in the cellular (platelets) and soluble components (plasma proteins) of blood. Platelet activation and induction of the intrinsic pathway of plasma coagulation are common mechanisms of NP-induced clotting enhancement, which is particularly dangerous for individuals suffering from hypercoagulable states associated with common diseases such as cancer, atherosclerosis, diabetes, and obstructive pulmonary disease[38].

Therefore, in the present work, the hemostatic potential of IY-AgNPs was assessed by the performance of a blood clotting test. The blood clotting activity of IY-AgNPs at different concentrations is shown in Fig. 5A–E. Compared to the control sample (Fig. 5A), IY-AgNPs at concentrations 500 and 1000 µg/mL (Fig. 5C,D) can efficiently shorten the blood clotting time. As shown in Fig. 5B, IY-AgNPs at concentrations 250 µg/mL no had a significant effect on the blood clotting time and their action was like to control sample. Thus, it can be observed that with an increase in the concentration of IY-AgNPs the efficiency of blood clotting was increased. However, IY-AgNPs effectively decreased clotting time at the highest concentrations by a 6 min decrease compared to control (Fig. 5E). The size, morphological feature, charge, chemical composition or type of cover and intrinsic characteristics of IY-AgNPs influence their hemostatic potential and the formation of blood clots[39]. In previous study, we reported that these NPs synthesized under sunlight irradiation reduced clotting time over 13 min at concentrations 500 and 1000 µg/mL compared to control[40]. This can be due to the synthesis of NPs in different conditions.

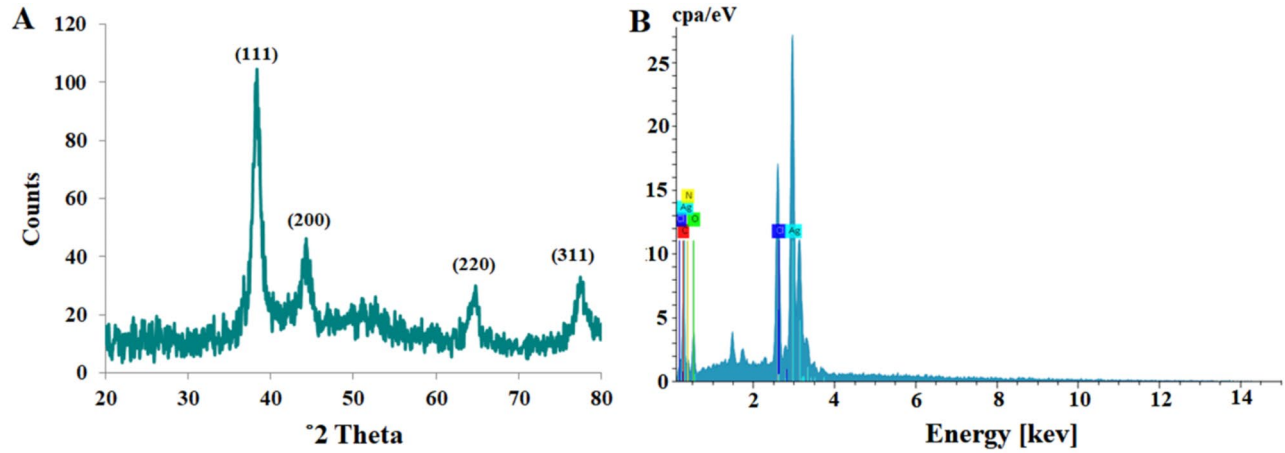

Fig. 4. XRD pattern (**A**) and EDX spectrum (**B**) of IY-AgNPs.

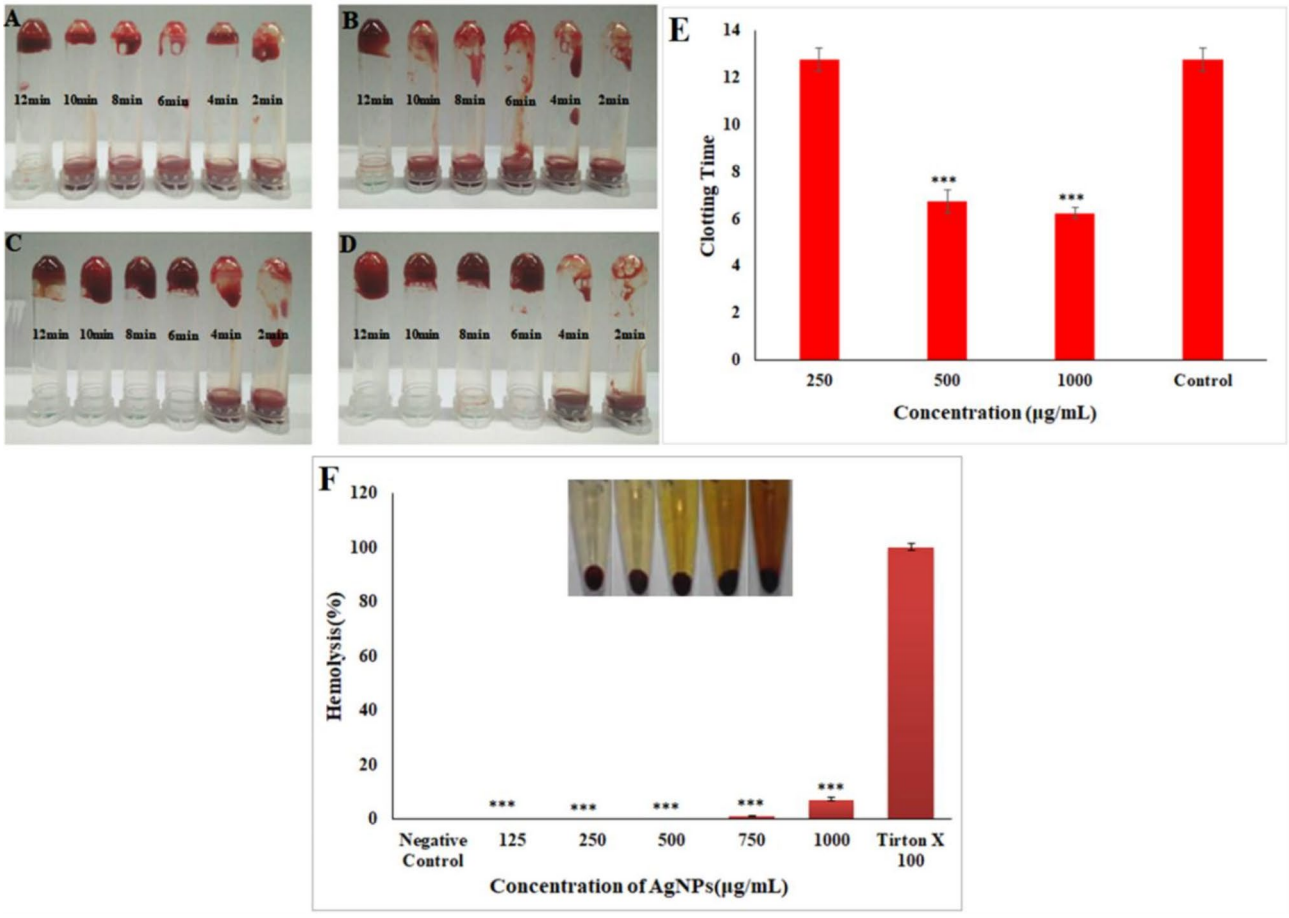

Fig. 5. The images of in vitro blood clotting time assay of normal saline as control (**A**) and IY-AgNPs at concentrations (**B**) 250 µg/mL, (**C**) 500 µg/mL and (**D**) 1000 µg/mL. (**E**) Blood clotting time graph, and (**F**) hemolytic activities of IY-AgNPs at different concentrations. Statistical differences between the test samples and control were obtained by Tukey's test, and significance was calculated at $p \leq 0.05$ (*** < 0.001, ** < 0.01, and * <0.05).

Also, Madhumathi et al., and Kumar et al., (2010), reported that b-chitin/nanosilver composite scaffolds showed more blood-clotting capability by shorting the blood clotting time due to the incorporation of AgNPs into their structures[41,42]. Based on these reported results, the reason for reducing blood-clotting time due to the presence of AgNPs is because of Ag potential in denaturation of the anticoagulant proteins and its effect on the intrinsic pathway of blood coagulation by creating a shortened clotting time[41–43]. In addition, as stated the physicochemical properties of NPs can influence the components of the coagulation system[44]. For example, the shape and sizes of NPs (< 100 nm) by higher penetration ability lead to fast cellular uptake and contact activation of coagulation factors and, also, surface charge of NPs can stimulate cell membrane destruction or change protein interactions that relate to contact activation or depletion of coagulation factors[45].

The reaction of NPs with RBCs can cause hemolysis, increase RBCs aggregation or decrease RBCs deformability, which may lead to inhibition of RBCs from performing their basic roles in hemostasis[46]. Therefore, hemolysis is an essential parameter in the hemocompatibility testing of NPs and can hold significant implications for their clinical applications[47]. The hemolytic effect of IY-AgNPs on RBCs has been shown in Fig. 5F. The obtained results revealed a low induced hemolytic action of IY-AgNPs on RBCs at higher concentrations. As shown in Fig. 5F, the RBCs lysis was only 0.96% and 7.13% at concentrations 750 and 1000 µg/mL, respectively compared to Triton X-100 with 100% hemolysis as a positive control. While no hemolysis occurred at other concentrations 125, 250 and 500 µg/mL like negative controls (normal saline). In the current research synthesized IY-AgNPs was very hemocompatible compared to our previous report for green synthesized AgNPs using *A. wilhelmsii* extract under sunlight irradiation by 12.84% hemolysis at concentration 1000 µg/mL[40]. This can be due to more negatively surface charge of IY-AgNPs. Halbandge et al. (2017) report that *Polyalthia longifolia* mediated AgNPs with size range 50–70 nm created 70% and 99% hemolytic effect at 50 and 100 µg/mL, respectively[48]. In addition, chemically synthesized and coated AgNPs using polyvinylpyrrolidone and sodium citrate induced 16.34% and 16.67% hemolysis with size 10 nm, respectively and 19% and 10% hemolysis, with size 20 nm, respectively at a concentration of 40 µg/mL[18,49].

The physicochemical properties of AgNPs such as size, charges, surface chemistry, coating agents and localized-SPR effect play a critical role in their toxicity effects[17]. For example, the smaller size of AgNPs < 50 nm than that of the bigger size of 50–100 nm makes greater hemolysis by increasing their uptake and membrane injury of RBCs[50], as well as positively charged AgNPs are more toxic than those with the negatively charged owing to their higher attraction to negatively surface charged RBCs[51]. Additionally, the interaction of negatively charged AgNPs with cations present in RBC membrane may also contribute to RBCs lysis[49]. The hemolytic activity of AgNPs attributed to their direct interaction with RBCs, the release of free Ag ions and also a combination of both actions, thus, these particles with high affinity can bind to thiol groups of proteins or phospholipids of the membrane, which ultimately lead to their denaturation and damage of membrane activity[50]. However, very low toxicity or hemolytic effects of IY-AgNPs on RBCs with excellent membrane stabilization activity and inhibition of protein denaturation can be due to their negatively surface charge and their coating agents, which are obtained from biomolecules existing in the IY extract.

In vitro anti-inflammatory potential assay

The anti-inflammatory potential of the IY-AgNPs was studied by determining the membrane stabilization and protein denaturation inhibition methods (Fig. 6).

Assay of inhibition of protein denaturation

The anti-inflammatory activity of the IY-AgNPs was studied by determining the inhibition of protein denaturation and membrane stabilization methods (Fig. 6). High temperatures lead to the denaturation of proteins through the destructive of their secondary and tertiary construction[52]. Denaturation of proteins is one

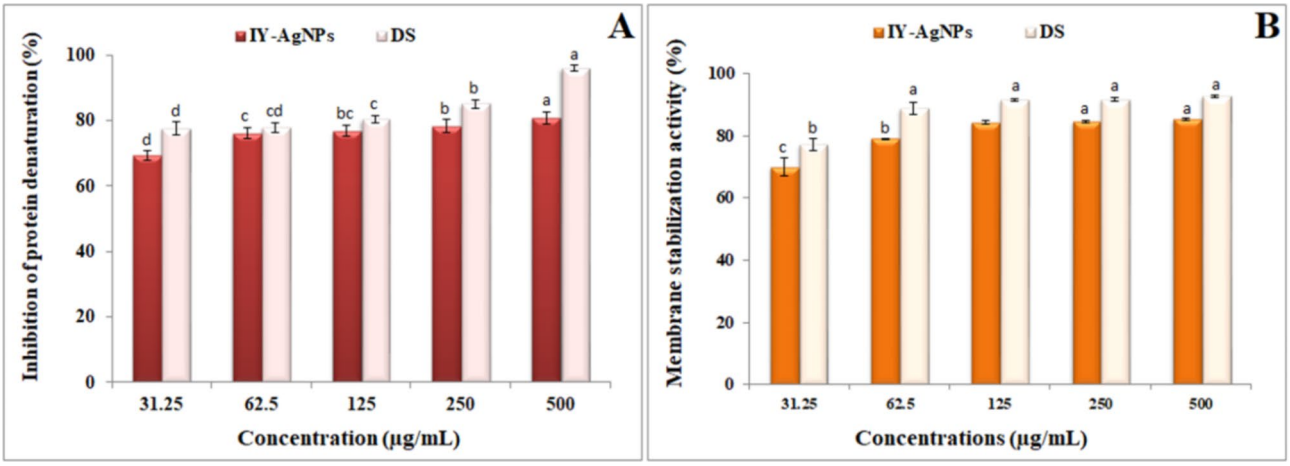

Fig. 6. Effect of IY-AgNPs on inhibiting the denaturation of BSA (**A**) and stabilizing membrane (**B**) at diverse concentrations of 31.25, 62.5, 125, 250, and 500 µg/mL compared to the reference drug of DS. The alphabetic symbols above each data set represent the statistical differences ($p < 0.05$, $n = 3$).

of the reasons for inflammation[53]. Anti-inflammatory drugs or appropriate inhibiting agents can be inhibited protein denaturation[52].

In the present study, the potential of synthesized IY-AgNPs in inhibiting of protein denaturation was investigated by inhibiting the heat-induced albumin denaturation. The inhibition percentage of protein denaturation of IY-AgNPs at concentrations ranging from 31.25 to 500 µg/mL was within the range from 69.3 to 80.7% (Fig. 6A), which revealed high anti-inflammatory activity by preventing the heat-induced albumin denaturation. The highest percentage of inhibition was 81% at a concentration of 500 µg/mL compared to DS drug with 96% at the same concentration. Anandhi et al. (2019) reported that green synthesized AgNPs from two plant species of *Chromolaena odorata* and *Caesalpinia coriari* indicated the maximum inhibition of protein denaturation of 74.35% and 56.24% at the concentration of 1000 µg/mL[54]. In addition, the inhibition percentage of protein denaturation using biological synthesized AgNPs from *Avicennia marina* reported 72.1%[55]. Compared to previously reported results, synthesized IY-AgNPs in our study can be an excellent anti-inflammatory agent by inhibiting protein denaturation.

Membrane stabilization

Lysis of red blood cells (RBCs) and oxidation of hemoglobin by their membrane rupture occurred when these cells are exposed to the hypotonic solution and increase the accumulation of fluid within cells, which these processes leads to leakage of serum proteins and fluids into tissues and thus, causes inflammation[54]. In the membrane stabilization assay, the RBCs are tested with several hemolytic stimuli such as heat, free radicals and osmotic shock[56]. The heat or hypotonicity-induced hemolysis of RBCs is widely used as a simple, rapid, sensitive and economic technique for the determination of anti-inflammatory properties of drugs[31]. The stabilization of RBCs from lysis can be related to the anti-inflammatory properties of a drug[53]. In the current research, all the tested concentrations of IY-AgNPs were exhibited significant membrane stabilizing activity at a concentration from 31.25 to 500 µg/mL (Fig. 6B). The IY-AgNPs at 500 µg/mL indicated maximum human RBCs membrane stabilization activity by 85.2%, compared to standard reference drug at the same concentration that showed 92.4% stabilization (Fig. 6B). Similarly, Govindappa et al. (2018), reported that the CtAgNPs (synthesis using *Calophyllum tomentosum* leaf extract) showed RBCs membrane stabilization by 84.18% [57]. Furthermore, biosynthesized AgNPs from the ethanol extract of *C. odorata*, *C. coriaria* (Bark) and *C. coriaria* (Leaves) showed 26%, 44% and 50%, respectively membrane stabilization activity[54]. Therefore, IY-AgNPs can be used as potent membrane stabilizers, which is near to diclofenac sodium as a standard drug.

Cytotoxic effects of optimized IY-AgNPs

Cytotoxicity experiments of the optimized IY-AgNPs were performed in the A375 and MCF-7 cancer cell lines using an MTT assay after 48 h of incubation. The attained results are shown in Fig. 7. It was observed that IY-AgNPs have significant cytotoxic effects on A375 and MCF-7 cells. The viability of A375 cells treated with IY-AgNPs remarkably decreased from 48.3 to 26.7% at concentration ranges of 12.5–100 µg/mL (Fig. 7A). The IC50 of IY-AgNPs was below 12.5 µg/mL against A375 cells. In the case of IY-extract, the viability of A375 cells was also diminished, and the IC50 value for it was up to 100 µg/mL (Fig. 7A). In the study by Das et al. (2013), the calculated IC50 values for different green synthesized TiO_2NPs (size ranges about 91–123 nm) using *Phytolacca decandra*, *Gelsemium sempervirens*, *Gelsemium canadensis*, *Thuja occidentalis* were 78, 80, 100 and 120 µg/mL, respectively against A375 cells[58]. Compared to this study, IY-AgNPs with an IC50 value of less than 12.5 µg/mL showed a higher cytotoxic effect against A375 cancer cells. The high cytotoxic effect of IY-AgNPs may be owing to its size and capping of IY phytochemicals such as phenolic compounds or proteins on the surface of these

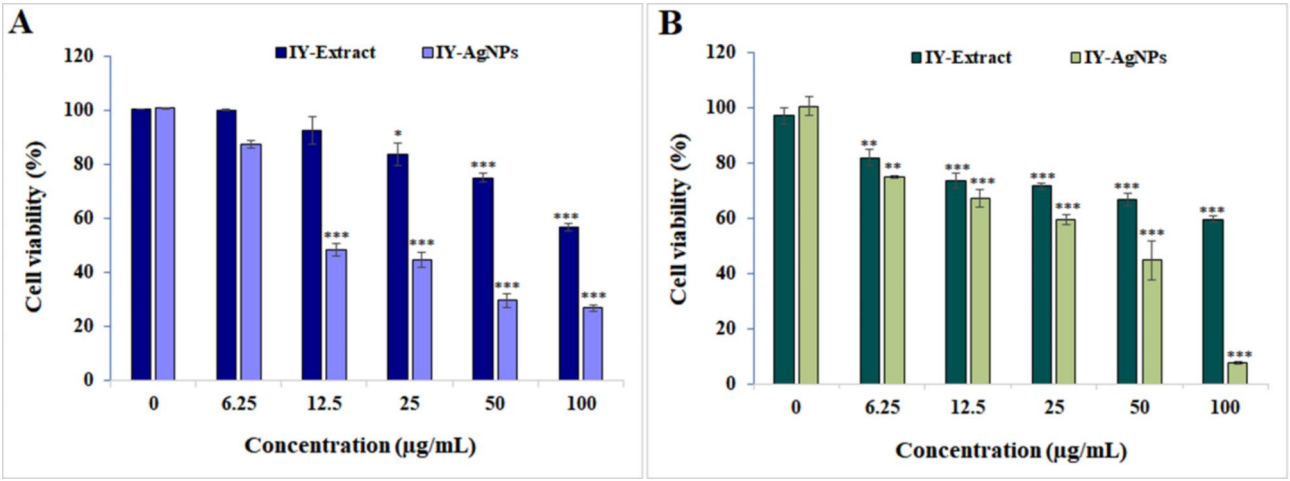

Fig. 7. Cytotoxic effects of biosynthesized IY-AgNPs and IY-extract on cancer cells of A375 (**A**) and MCF-7 (**B**) at diverse concentrations (6.25, 12.5, 25, 50 and100 µg/mL) relative to the untreated control (0 µg/mL). Statistical differences between the test samples and control were obtained by Tukey's test, and significance was calculated at $p \leq 0.05$ (*** < 0.001,* * < 0.01, and* <0.05).

particles. In line with our study, Francis et al. (2018) reported that green synthesized AgNPs using leaf extract of *Elephantopus scaber* (diameter of 37.86 nm) caused IC50 value of 15.68 ± 0.15 µg/mL on A375 cells[59].

We have also evaluated the cytotoxic potential of IY-AgNPs against the MCF-7 cancer cell line (Fig. 7B). As observed in Fig. 7B, the MCF-7 cell viability remarkably reduced from 75% to 7.7 against IY-AgNPs in the concentration range of 6.25–100 µg/mL. The IC50 value of IY-AgNPs was between 25 and 50 µg/mL against MCF-7 cells. Also, in MCF-7 cells in the presence of IY-extract, high cytotoxicity was observed at the highest concentration of 100 µg/mL (viability 59.6%). Therefore, according to the analyzed results, IY-AgNPs demonstrated higher cytotoxic effects on A375 and MCF-7 cells than IY-extract. Similarly, Acacia lignin mediated silver nanoparticles (10–50 nm, spherical) demonstrated 20–30% toxicity effects in MCF-7 and A375 cancer cells at concentrations of 5–500 µg/mL[60]. Moreover, consistent with our study, Mariadoss et al.(2019) indicated the cytotoxicity impact of biosynthesized AgNPs using *Mallus domestica* (50–107.3 nm) on cell growth of MCF-7 cells at different concentrations of 10–100 µg/mL with the IC 50 value of 33.81 µg/mL[61]. Therefore, physicochemical properties of AgNPs, such as their size and capping or stabilizing agent on the surface of nanoparticles, play an important role in inducing cytotoxicity[62].

The abnormal metabolism and higher uptake of AgNPs by cells can be the reason for the selective cytotoxicity of green synthesized AgNPs against cancer cells[63]. The green synthesized AgNPs efficiently interact with cancer cells due to their highly porous structure and higher permeability and retention impact. This leads to the production of reactive oxygen species, which cause oxidative stress, impaired cellular respiration, mitochondrial dysfunction, DNA damage, apoptosis, and thus inhibit the cancer cell proliferation and survival by upregulating and downregulating the physiological signaling pathways[64].

DPPH radical scavenging activity

The antioxidant effects of IY-AgNPs and IY-extract were analyzed by measuring the percentage of DPPH radical inhibition. The deep purple color of the DPPH radical is due to its odd electrons. Antioxidant compounds lead to the decolonization of DPPH radical by donating electrons, which these changes can be quantitatively measured by absorbance[65]. As shown in Fig. 8, the antioxidant activity of IY-AgNPs increased with increasing their concentration. Significant differences were observed between IY-AgNPs and IY-extract in DPPH radical inhibition activity. In this regard, IY-AgNPs at concentrations of 150–350 µg/mL revealed a scavenging percentage

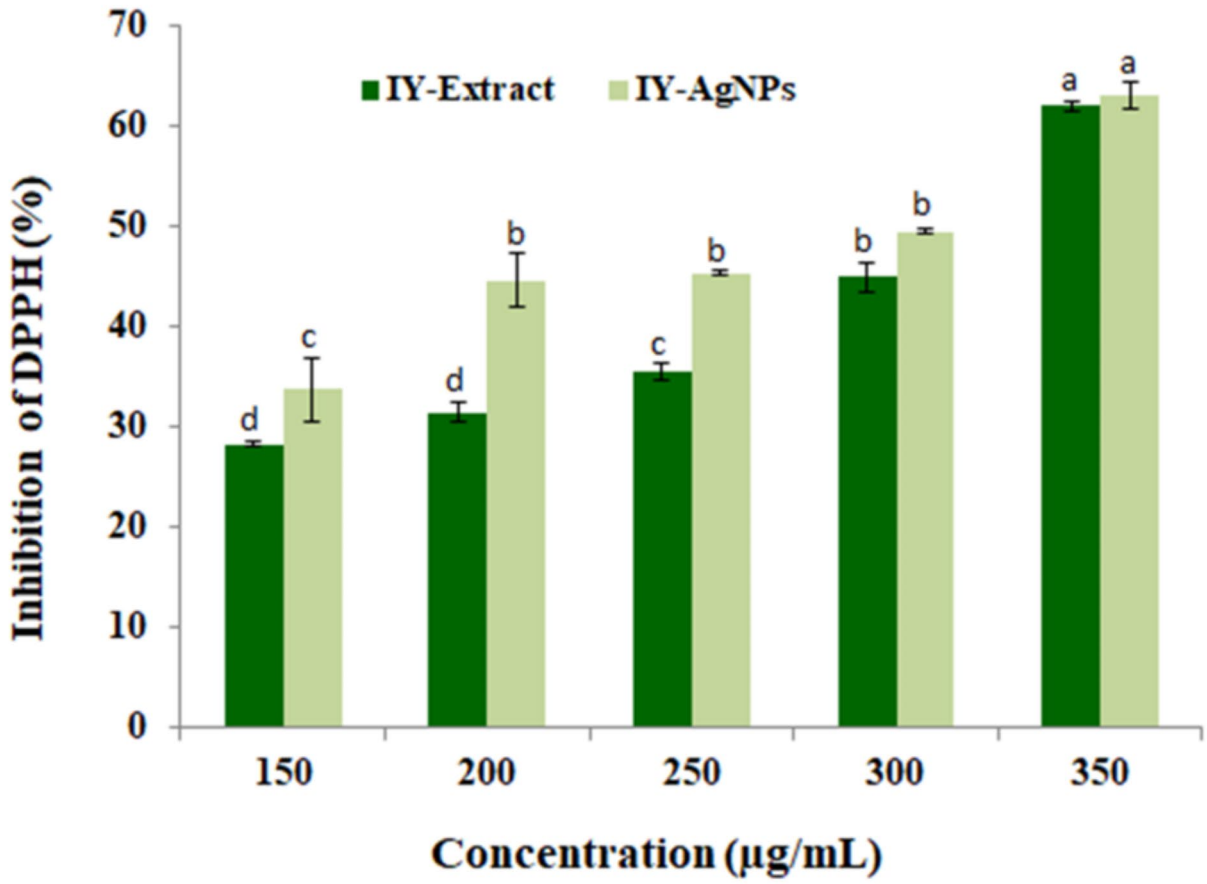

Fig. 8. The antioxidant effects of the biosynthesized IY-AgNPs and IY-extract at various concentrations of 150–350 µg/mL. The alphabetic symbols above each column represent the statistical differences ($p < 0.05$, $n = 3$).

Microorganisms	IY-AgNPs	
	MIC (µg/mL)	MBC/MFC (µg/mL)
S. aureus	25	50
E. coli	100	100
P. aeruginosa	200	200
C. albicans	200	200

Table 1. Bactericidal and fungicidal effects of IY-AgNPs.

of 33.8–63.2% in response to DPPH (Fig. 8). The highest DPPH scavenging activity of IY-AgNPs and IY-extract at a concentration of 350 µg/mL was 63.2% and 62.1%, respectively. IY-AgNPs showed higher scavenging activity in than the IY-extract because of the existence of biological compounds on the AgNPs surface. A similar result was reported about green synthesized spherical AgNPs (32 nm) from *Pistacia terebinthus* extract with the highest DPPH scavenging activity of 64.3% at a concentration of 400 µg/mL[66]. Therefore, IY-AgNPs as a potent antioxidant can be new hope for application in the medical and pharmaceutical industry.

Microbiocidal effects of IY-AgNPs

Tested microorganisms in the present study, especially *S. aureus*, *P. aeruginosa*, *E. coli*, and *C. albicans*, are the most common cause of skin or wound site infections and hospital-acquired systemic infections, which can be a problem for patients and health services. *S. aureus* is the most common cause of cutaneous and systemic infections, and diseases include impetigo and ecthyma, erysipelas, cellulitis, necrotizing fasciitis, folliculitis, furunculosis, and carbunculosis, scalded skin syndrome, and toxic shock syndrome[67]. Moreover, *P. aeruginosa* may cause cutaneous infection and diseases such as ecthyma gangrenosum in immunosuppressed patients, gram-negative toe web infections, and green nail syndrome, as well as is a cause of mortality and morbidity in burn victims[67]. Additionally, *E. coli* is another common pathogen, which is found in the original site of infection, wound area, and bloodstream[32].

C. albicans is a member of the healthy microbiota, which with alterations in host immunity, stress, resident microbiota, etc. colonizing the reproductive tract, gastrointestinal tract, oral cavity, and skin and causing superficial infections; including oral or vaginal candidiasis and life-threatening systemic infections, bloodstream infections in clinical settings, 15% of all hospital-acquired sepsis and medical device infections (venous catheters, joint prostheses, mechanical heart valves, pacemakers, dentures, and contact lenses)[68,69]. Thus, to deal with these pathogens or bacterial resistance towards the currently used antibiotics, using AgNPs as a remarkable antimicrobial agent may be a choice for monitoring the proliferation of human pathogens.

In this research, bactericidal effects of IY-AgNPs were determined on a gram-positive bacterium *S. aureus* and a gram-negative bacteria *E. coli* and *P. aeruginosa*, as well as their fungicidal effect was investigated on *C. albicans* using the MIC microdilution method. In addition, the MBC value for bacterial pathogens and the MFC value for fungal pathogen were evaluated. MIC, MBC, and MFC of IY-AgNPs have been revealed in Table 1. Based on the achieved results, MIC of IY-AgNPs was 25 µg/mL for *S. aureus*, 100 µg/mL for *E. coli*, and 200 µg/mL for *P. aeruginosa* and *C. albicans*. As shown in Table 1, the maximum bactericidal effects of IY-AgNPs were against *S. aureus* with MIC 25 µg/mL and MBC 50 µg/mL compared to other pathogens. MBC value *S. aureus* was higher than that of MIC value and for other strains was similar to their MIC values. The different bactericidal effects of IY-AgNPs against selected bacteria may depend on their spherical shape, small size, coating agents, and the bacterial strains.

Compared to the good bactericidal effects of IY-AgNPs in our research, Rashid et al. (2019) reported that biosynthesized AgNPs using roots extract of *Rumex hastatus*, *Rumex dantatus*, *Bergenia stracheyi*, and *Bergenia ciliata*, showed antibacterial effects with MIC values 250, 250, 750 and 1000 µg/mL, respectively against *P. aeruginosa* and, 250, 250, 500 and 750 µg/mL, respectively, against *S. aureus* with an MBC values of 1–3 mg/mL[37]. Also, in their study, MIC of *R. hastatus* and *R. dantatus* based AgNPs calculated 250 and 500 µg/mL, respectively against *E. coli* with MBC of 2 mg/mL[37]. Furthermore, Bagherzadeh et al. (2017) investigated the comparison of bactericidal effects of biosynthesized AgNPs using saffron extract with size 12–20 nm and purchased AgNPs (chemically synthesized) with size 15 nm against six pathogenic bacteria such as *S. aureus*, *E. coli*, *P. aeruginosa*, *Klebsiella pneumonia*, *Shigella flexneri*, and *Bacillus subtilis*, and their results indicated that the purchased AgNPs did not have a significant antibacterial effect, but biosynthetic AgNPs with MIC of 250 µg/mL were able to inhibit the growth of these bacteria except for *S. aureus*[70]. Therefore, newly biogenic synthesized IY-AgNPs using aqueous extract of IY, as a safe and cost-effective method, can be considered as a promising antimicrobial agent or an effective solution against serious problems of resistant bacterial pathogens or newer bacterial strains and applied for the treatment of infectious diseases. In addition to microbiocidal properties, these NPs have antioxidant, anti-inflammatory, anti-bleeding/anti-ulcer and anti-hemolytic effects, which can prove their ability to treat and heal wounds and various diseases without causing inflammation.

Conclusion

The prepared and stabilized IY-AgNPs using yarrow extract under optimal conditions (at a pH 10 and a temperature of 70 °C) were characterized by UV, FT-IR, TEM, and XRD. The XRD and TEM studies showed crystalline nature, spherical morphology, and an average particle size of 19. 25 ± 7.9 nm of IY-AgNPs. FTIR analysis showed involving yarrow extract biomolecules as reducing and stabilizing agents in the formation of NPs. These particles showed significant antioxidant activity and strongly prevented bacterial (particularly *S.*

aureus) and fungal growth, which demonstrated the role of IY-AgNPs as an antimicrobial agent. The synthesized IY-AgNPs as an excellent anti-inflammatory agent significantly inhibited the protein denaturation (up to 80%) and stabilized RBCs from lysis. The blood-clotting time assay of particles showed that the IY-AgNPs, clots the blood rapidly compared to the control drug. Furthermore, IY-AgNPs exhibited potent cytotoxic effects against cancer cells of A375 and MCF-7 relative to pure IY-extract. The described effects were partly material specific, suggesting that in addition to size and shape, the surface charge, coat and topology may be more relevant for blood compatibility or other biological activity of NPs. However, founded results demonstrated that IY-AgNPs with anti-inflammatory, antioxidant, anti-microbial, anticancer and anti-bleeding ability can be applied to treat various diseases and for wound healing. Also, they may significantly contribute to the design of therapies and drug delivery systems and can solve the problems and side effects of common chemical drugs. Future in vivo studies are necessary to elucidate the molecular mechanisms involved in blood biocompatibility, anti-inflammatory, anticancer and wound healing activity of IY-AgNPs.

Data availability

The datasets generated during and/or analyzed during the current study are available from the corresponding author on reasonable request.

Received: 14 September 2024; Accepted: 4 December 2024
Published online: 07 January 2025

References

1. Fahed, L., Beyrouthy, E., Ouaini, M., Eparvier, N., Stien, D. & V. & Isolation and characterization of santolinoidol, a bisabolene sesquiterpene from *Achillea santolinoides* subsp wilhelmsii (K. Koch) Greuter. *Tetrahedron. Lett.* **57**, 1892–1894 (2016).
2. Akkol, E. K., Koca, U., Pesin, I. & Yilmazer, D. Evaluation of the wound healing potential of *Achillea biebersteinii* Afan.(Asteraceae) by in vivo excision and incision models. *Evid.-Based Complement. Altern. Med.* **2011** (2011).
3. Amjad, L., Mohammadi-Sichani, M. & Mohammadi-Kamalabadi, M. Potential activity of the *Achillea wilhelmsii* leaves on bacteria. *Int. J. Biosci. Biochem. Bioinform.* **1**, 216 (2011).
4. Dias, M. I. et al. Chemical composition of wild and commercial *Achillea millefoliu*m L. and bioactivity of the methanolic extract, infusion and decoction. *Food Chem.* **141**, 4152–4160 (2013).
5. Alfatemi, S. M. H., Rad, J. S., Rad, M. S., Mohsenzadeh, S. & da Silva, J. A. T. Chemical composition, antioxidant activity and in vitro antibacterial activity of *Achillea Wilhelmsii* C. Koch essential oil on methicillin-susceptible and methicillin-resistant Staphylococcus aureus spp. *3 Biotech.* **5**, 39–44 (2015).
6. Saeidnia, S., Gohari, A. R., Mokhber-Dezfuli, N. & Kiuchi, F. A review on phytochemistry and medicinal properties of the genus Achillea. *DARU J. Fac. Pharm. Tehran Univ. Med. Sci.* **19**, 173 (2011).
7. Khazneh, E. et al. The chemical composition of *Achillea Wilhelmsii* C. Koch and its desirable effects on hyperglycemia, inflammatory mediators and hypercholesterolemia as risk factors for cardiometabolic disease. *Molecules* **21**, 404 (2016).
8. Ashtiani, M. et al. Effect of *Achillea Wilhelmsii* extract on expression of the human telomerase reverse transcriptase mRNA in the PC3 prostate cancer cell line. *Biomed. Rep.* **7**, 251–256 (2017).
9. Sargazi, S., Moudi, M., Kooshkaki, O., Mirinejad, S. & Saravani, R. Hydro-alcoholic extract of *Achillea Wilhelmsii* C. Koch reduces the expression of cell death-associated genes while inducing DNA damage in HeLa cervical cancer cells. *Iran. J. Med. Sci.* **45**, 359 (2020).
10. Saravani, R., Galavi, H. R. & Shahraki, A. Inhibition of phosphodiesterase 5 and increasing the level of cyclic guanosine 3′, 5′ monophosphate by hydroalcoholic *Achillea Wilhelmsii* C. Koch extract in human breast cancer cell lines MCF-7 and MDA-Mb-468. *Breast Cancer Basic. Clin. Res.* **11**, 1178223417690178 (2017).
11. Suzergoz, F., Cinar, S., Oktay, R., Karakus, F. & Gurol, A. O. Effect of the *Achillea wilhelmsii* extract intake upon blood lipid profile, haematologic and immunologic parameters in the rat. *Food Agric. Immunol.* **26**, 46–59 (2015).
12. Tadić, V. et al. The estimation of the traditionally used yarrow (*Achillea millefolium* L. Asteraceae) oil extracts with anti-inflamatory potential in topical application. *J. Ethnopharmacol.* **199**, 138–148 (2017).
13. Augustine, R. & Hasan, A. Emerging applications of biocompatible phytosynthesized metal/metal oxide nanoparticles in healthcare. *J. Drug Deliv Sci. Technol.* 101516 (2020).
14. Mousavi-Khattat, M., Keyhanfar, M. & Razmjou, A. A comparative study of stability, antioxidant, DNA cleavage and antibacterial activities of green and chemically synthesized silver nanoparticles. *Artif. Cells Nanomed. Biotechnol.* **46**, S1022–S1031 (2018).
15. Ravichandran, V. et al. Green synthesis, characterization, antibacterial, antioxidant and photocatalytic activity of *Parkia speciosa* leaves extract mediated silver nanoparticles. *Results Phys.* **15**, 102565 (2019).
16. Liu, T. et al. The effect of size and surface ligands of iron oxide nanoparticles on blood compatibility. *RSC Adv.* **10**, 7559–7569 (2020).
17. Ashokraja, C., Sakar, M. & Balakumar, S. A perspective on the hemolytic activity of chemical and green-synthesized silver and silver oxide nanoparticles. *Mater. Res. Express*. **4**, 105406 (2017).
18. Huang, H. et al. An evaluation of blood compatibility of silver nanoparticles. *Sci. Rep.* **6**, 25518 (2016).
19. Hamouda, R. A., Hussein, M. H., Abo-elmagd, R. A. & Bawazir, S. S. Synthesis and biological characterization of silver nanoparticles derived from the cyanobacterium *Oscillatoria limnetica*. *Sci. Rep.* **9**, 1–17 (2019).
20. Ahn, E. Y. & Park, Y. Anticancer prospects of silver nanoparticles green-synthesized by plant extracts. *Mater. Sci. Eng. C* **111253** (2020).
21. Kaplan, Ö. et al. Biosynthesis and characterization of silver nanoparticles from Tricholoma Ustale and Agaricus Arvensis extracts and investigation of their antimicrobial, cytotoxic, and apoptotic potentials. *J. Drug Deliv. Sci. Technol.* **69**, 103178 (2022).
22. Ibraheem, D. R. et al. Ciprofloxacin-loaded silver nanoparticles as potent nano-antibiotics against resistant pathogenic bacteria. *Nanomaterials*. **12**, 2808 (2022).
23. Jangid, H., Singh, S., Kashyap, P., Singh, A. & Kumar, G. Advancing biomedical applications: an in-depth analysis of silver nanoparticles in antimicrobial, anticancer, and wound healing roles. *Front. Pharmacol.* **15**, 1438227 (2024).
24. Pereira, T. M., Polez, V. L. P., Sousa, M. H. & Silva, L. P. Modulating physical, chemical, and biological properties of silver nanoparticles obtained by green synthesis using different parts of the tree *Handroanthus heptaphyllus* (Vell.) Mattos. *Colloid Interface Sci. Commun.* **34**, 100224 (2020).
25. Odeniyi, M. A., Okumah, V. C., Adebayo-Tayo, B. C. & Odeniyi, O. A. Green synthesis and cream formulations of silver nanoparticles of *Nauclea latifolia* (African peach) fruit extracts and evaluation of antimicrobial and antioxidant activities. *Sustain. Chem. Pharm.* **15**, 100197 (2020).
26. Pirtarighat, S., Ghannadnia, M. & Baghshahi, S. Green synthesis of silver nanoparticles using the plant extract of *Salvia spinosa* grown in vitro and their antibacterial activity assessment. *J. Nanostruct. Chem.* **9**, 1–9 (2019).

27. Mani, A. K. M., Seethalakshmi, S. & Gopal, V. Evaluation of in-vitro anti-inflammatory activity of silver nanoparticles synthesised using *piper nigrum* extract. *J. Nanomed. Nanotechnol.* **6**, 1 (2015).
28. Marcato, P. D. et al. In vivo evaluation of complex biogenic silver nanoparticle and enoxaparin in wound healing. *J. Nanomater.* **2015** (2015).
29. Ginwala, R., Bhavsar, R., Chigbu, D. G. I., Jain, P. & Khan, Z. K. Potential role of flavonoids in treating chronic inflammatory diseases with a special focus on the anti-inflammatory activity of apigenin. *Antioxidants* **8**, 35 (2019).
30. Joshi, B. B., Chaudhari, M. G. & Mistry, K. N. In vitro screening of anti-inflammatory and anti-diabetic activity of stem bark of *Bauhinia purpurea*. *J. Pharm. Biomed. Sci.*. **37**, 1964–1919 (2013).
31. Ogbomade, R. S., Asara, A. A. & Eboh, A. In vitro anti-inflammatory properties of leaf extract of *Polyalthia longifolia* extract. *Pharm. Chem. J.* **6**, 80 (2019).
32. Giri, V. P. et al. Biogenic silver nanoparticles as a more efficient contrivance for wound healing acceleration than common antiseptic medicine. *FEMS Microbiol. Lett.* **366**, fnz201 (2019).
33. Ratnayake, W., Suresh, T. S., Abeysekera, A. M., Salim, N. & Chandrika, U. G. Acute anti-inflammatory and anti-nociceptive activities of crude extracts, alkaloid fraction and evolitrine from *Acronychia pedunculata* leaves. *J. Ethnopharmacol.* **238**, 111827 (2019).
34. Zhang, Y. et al. A highly elastic and rapidly crosslinkable elastin-like polypeptide-based hydrogel for biomedical applications. *Adv. Funct. Mater.* **25**, 4814–4826 (2015).
35. Vijayakumar, S. et al. Garlic clove extract assisted silver nanoparticle–antibacterial, antibiofilm, antihelminthic, anti-inflammatory, anticancer and ecotoxicity assessment. *J. Photochem. Photobiol. B Biol.* **198**, 111558 (2019).
36. Serino, E. et al. Salvigenin, a trimethoxylated flavone from *Achillea Wilhelmsii* C. Koch, exerts combined lipid-lowering and mitochondrial stimulatory effects. *Antioxidants* **10**, 1042 (2021).
37. Rashid, S., Azeem, M., Khan, S. A., Shah, M. M. & Ahmad, R. Characterization and synergistic antibacterial potential of green synthesized silver nanoparticles using aqueous root extracts of important medicinal plants of Pakistan. *Colloids Surf. B Biointerfaces*. **179**, 317–325 (2019).
38. Fröhlich, E. Action of nanoparticles on platelet activation and plasmatic coagulation. *Curr. Med. Chem.* **23**, 408–430 (2016).
39. De La Cruz, G. G. et al. Interaction of nanoparticles with blood components and associated pathophysiological effects. *Unraveling Saf. Profile Nanoscale Part. Mater. Biomed. Environ. Appl.* (2018).
40. Chahrdoli, A. et al. *AchWilhelmsiielmsii* C. Koch mediated blood compatible silver nanoparticles. *Mater. Today Commun.* **25**, 101577 (2020).
41. Kumar, P. T. S. et al. Preparation and characterization of novel β-chitin/nanosilver composite scaffolds for wound dressing applications. *Carbohydr. Polym.* **80**, 761–767 (2010).
42. Madhumathi, K. et al. Development of novel chitin/nanosilver composite scaffolds for wound dressing applications. *J. Mater. Sci. Mater. Med.* **21**, 807–813 (2010).
43. Lu, Z. et al. Enhanced antibacterial and wound healing activities of microporous chitosan-Ag/ZnO composite dressing. *Carbohydr. Polym.* **156**, 460–469 (2017).
44. Sun, H. et al. Nanotechnology-enabled materials for hemostatic and anti-infection treatments in orthopedic surgery. *Int. J. Nanomed.* **13**, 8325 (2018).
45. Ilinskaya, A. N. & Dobrovolskaia, M. A. Nanoparticles and the blood coagulation system. Part II: safety concerns. *Nanomedicine* **8**, 969–981 (2013).
46. de la Harpe, K. M. et al. The hemocompatibility of nanoparticles: a review of cell–nanoparticle interactions and hemostasis. *Cells* **8**, 1209 (2019).
47. Krajewski, S. et al. Hemocompatibility evaluation of different silver nanoparticle concentrations employing a modified Chandler-loop in vitro assay on human blood. *Acta Biomater.* **9**, 7460–7468 (2013).
48. Halbandge, S. D., Mortale, S. P. & Karuppayil, S. M. Biofabricated silver nanoparticles synergistically activate amphotericin B against mature biofilm forms of *Candida albicans*. *Open. Nanomed. J.* **4**, (2017).
49. Ferdous, Z., Beegam, S., Tariq, S., Ali, B. H. & Nemmar, A. The in vitro effect of polyvinylpyrrolidone and citrate coated silver nanoparticles on erythrocytic oxidative damage and eryptosis. *Cell. Physiol. Biochem.* **49**, 1577–1588 (2018).
50. Chen, L. Q. et al. Nanotoxicity of silver nanoparticles to red blood cells: size dependent adsorption, uptake, and hemolytic activity. *Chem. Res. Toxicol.* **28**, 501–509 (2015).
51. Adragnaa, N. C. et al. Assessment of silver-nanoparticles-induced erythrocyte cytotoxicity through ion transport studies. *Cell. Physiol. Biochem.* **53**, 532–549 (2019).
52. Kamalakannan, R., Mani, G., Muthusamy, P., Susaimanickam, A. A. & Kim, K. Caffeine-loaded gold nanoparticles conjugated with PLA-PEG-PLA copolymer for in vitro cytotoxicity and anti-inflammatory activity. *J. Ind. Eng. Chem.* **51**, 113–121 (2017).
53. Ezzat, S. M., Ezzat, M. I., Okba, M. M., Menze, E. T. & Abdel-Naim, A. B. The hidden mechanism beyond ginger (*Zingiber officinale* Rosc.) Potent in vivo and in vitro anti-inflammatory activity. *J. Ethnopharmacol.* **214**, 113–123 (2018).
54. Anandhi, D., Kanaga, G., Jagatheesh, S. & Revathi, K. In vitro evaluation of biological activity (anti-inflammatory, antiarthritic, and antidiabetic) of green synthesized silver nanoparticles from ethanolic extract of *Chromolaena odorata*, *Caesalpinia coriaria* (bark and leaves). *Drug Invent. Today* **12**, (2019).
55. Kumaran, N. S. In vitro anti-inflammatory activity of silver nanoparticle synthesized *Avicennia marina* (Forssk.) Vierh.: a green synthetic approach. *Int. J. Green. Pharm.* **12**, (2018).
56. Takebayashi, J. et al. Inhibition of free radical-induced erythrocyte hemolysis by 2-O-substituted ascorbic acid derivatives. *Free Radic. Biol. Med.* **43**, 1156–1164 (2007).
57. Govindappa, M., Hemashekhar, B., Arthikala, M. K., Rai, V. R. & Ramachandra, Y. L. Characterization, antibacterial, antioxidant, antidiabetic, anti-inflammatory and antityrosinase activity of green synthesized silver nanoparticles using *Calophyllum tomentosum* leaves extract. *Results Phys.* **9**, 400–408 (2018).
58. Das, S. et al. Biosynthesized silver nanoparticles by ethanolic extracts of *Phytolacca decandra*, *Gelsemium sempervirens*, *Hydrastis canadensis* and *Thuja occidentalis* induce differential cytotoxicity through G2/M arrest in A375 cells. *Colloids Surf. B Biointerfaces*. **101**, 325–336 (2013).
59. Francis, S., Joseph, S., Koshy, E. P. & Mathew, B. Microwave assisted green synthesis of silver nanoparticles using leaf extract of elephantopus scaber and its environmental and biological applications. *Artif. Cells Nanomed. Biotechnol.* **46**, 795–804 (2018).
60. Aadil, K. R., Barapatre, A., Meena, A. S. & Jha, H. Hydrogen peroxide sensing and cytotoxicity activity of *Acacia lignin* stabilized silver nanoparticles. *Int. J. Biol. Macromol.* **82**, 39–47 (2016).
61. Mariadoss, A. V. A. et al. Green synthesis, characterization and antibacterial activity of silver nanoparticles by Malus domestica and its cytotoxic effect on (MCF-7) cell line. *Microb. Pathog.* **135**, 103609 (2019).
62. Remya, R. R., Rajasree, S. R. R., Aranganathan, L. & Suman, T. Y. An investigation on cytotoxic effect of bioactive AgNPs synthesized using *Cassia fistula* flower extract on breast cancer cell MCF-7. *Biotechnol. Rep.* **8**, 110–115 (2015).
63. Dutt, Y. et al. Silver nanoparticles phytofabricated through *Azadirachta indica*: anticancer, apoptotic, and wound-healing properties. *Antibiotics* **12**, 121 (2023).
64. Abdellatif, A. A. H., Mostafa, M. A. H., Konno, H. & Younis, M. A. Exploring the green synthesis of silver nanoparticles using natural extracts and their potential for cancer treatment. *3 Biotech.* **14**, 1–21 (2024).
65. Deepika, S., Selvaraj, C. I. & Roopan, S. M. Screening bioactivities of *Caesalpinia pulcherrima* L. Swartz and cytotoxicity of extract synthesized silver nanoparticles on HCT116 cell line. *Mater. Sci. Eng. C.* **106**, 110279 (2020).

66. Naghmachi, M. et al. Green synthesis of silver nanoparticles (AgNPs) by *Pistacia terebinthus* extract: Comprehensive evaluation of antimicrobial, antioxidant and anticancer effects. *Biochem. Biophys. Res. Commun.* (2022).
67. Chiller, K., Selkin, B. A. & Murakawa, G. J. Skin microflora and bacterial infections of the skin. *J. Investig. Dermatol. Symp. Proc.* **6**, 170–174 (2001).
68. Mayer, F. L., Wilson, D. & Hube, B. *Candida albicans* pathogenicity mechanisms. *Virulence* **4**, 119–128 (2013).
69. Nobile, C. J. & Johnson, A. D. *Candida albicans* biofilms and human disease. *Annu. Rev. Microbiol.* **69**, 71–92 (2015).
70. Bagherzade, G., Tavakoli, M. M. & Namaei, M. H. Green synthesis of silver nanoparticles using aqueous extract of saffron (*Crocus sativus* L.) wastages and its antibacterial activity against six bacteria. *Asian Pac. J. Trop. Biomed.* **7**, 227–233 (2017).

Acknowledgements
The authors gratefully acknowledge the Research Council of Kermanshah University of Medical Sciences.

Author contributions
A.C. contributed to the study conception and design, investigation, methodology, software, data collection and analysis, data interpretation, writing & editing. The project administration, resources, supervision, validation, and editing were performed by Y.S. and A.F. F.Q. and P.H. performed the blood compatibility tests. The first draft of the manuscript was written by A.C. and all authors commented on previous versions of the manuscript. All authors read and approved the final manuscript.

Funding
This research did not receive any specific grant from funding agencies in the public, commercial, or not-for-profit sectors.

Declarations

Competing interests
The authors declare no competing interests.

Additional information
Correspondence and requests for materials should be addressed to A.C., Y.S. or A.F.

Reprints and permissions information is available at www.nature.com/reprints.

Publisher's note Springer Nature remains neutral with regard to jurisdictional claims in published maps and institutional affiliations.